The 14th International Topical Meeting on Nuclear Reactor Thermalhydraulics, NURETH-14
Toronto, Ontario, Canada, September 25-30, 2011

NURETH14-286

COUPLED LARGE-EDDY SIMULATION OF THERMAL MIXING IN A T-JUNCTION

D. Kloeren[1,2] and E. Laurien[1]

[1] Institute for Nuclear Technology and Energy Systems (IKE), University of Stuttgart, Germany

[2] EnBW Kernkraft GmbH, Kernkraftwerk Neckarwestheim, Neckarwestheim, Germany

david.kloeren@ike.uni-stuttgart.de , eckart.laurien@ike.uni-stuttgart.de

Abstract

Analyzing thermal fatigue due to thermal mixing in T-junctions is part of the safety assessment of nuclear power plants. Results of two large-eddy simulations of mixing flow in a T-junction with coupled and adiabatic boundary condition are presented and compared. The temperature difference is set to 100 K, which leads to strong stratification of the flow. The main and the branch pipe intersect horizontally in this simulation. The flow is characterized by steady wavy pattern of stratification and temperature distribution. The coupled solution approach shows highly reduced temperature fluctuations in the near wall region due to thermal inertia of the wall. A conjugate heat transfer approach is necessary in order to simulate unsteady heat transfer accurately for large inlet temperature differences.

1. Introduction

Providing reliable fatigue analysis for components subjected to thermal cyclic loading is important for the safety analysis of nuclear power plants. One problem that has been under investigation in recent years is the T-junction mixing flow. In 1998 wall-through cracks was observed in the residual heat removal system in the French light water reactor Civaux I only after a few thousand hours. These cracks occurred due to high cycles of low frequency temperature fluctuations in the range of 1 to 10 Hz [1] In order to understand the mechanism of high cycle fatigue and provide reliable information about the lifetime of such components, accurate information about frequencies and the amplitude of temperature fluctuations are required.

Large-eddy simulations (LES) were performed to estimate thermal striping in a T-junction [2]-[7]. When non-adiabatic T-junction problems were investigated either the heat flux or the temperature was usually given at the boundaries [5]. Conjugate heat transfer calculations have been performed by Hannink et al.[6] and Kuhn et al. [7]. It was concluded that LES with coupled boundary condition is capable to simulate T-junction flow unsteady and conjugate heat transfer. Kuhn et al and Howard et al. [8] compared the conjugate heat transfer LES simulation with FATHERINO experiments, which provided temperature fields of the outer pipe wall surface.

Most experiments are designed for low inlet temperature differences in order to allow optical access for non-intrusive measurements for measurements of the velocity and temperature field. However, besides turbulent mixing both stratification and unsteady heat transfer effects have to be simulated correctly and validated against data in the pipe flow as well as inside the pipe wall. Therefore, a new experimental setup at the Institute of Nuclear Technology and Energy Systems (IKE) in

cooperation with the Material Testing Institute (MPA) is built to address the need for validation data under realistic conditions to investigate thermal fatigue. It is designed to allow a system pressure of 7.5MPa and temperatures up to 280°C. For this experiment the branch pipe intersects the main pipe horizontally. In this paper, first results of a blind calculation based on flow parameter and geometry of the experiment are presented. A conjugate heat transfer simulation is compared to an adiabatic boundary condition case to study the influence of the coupled approach.

2. Test case based on IKE thermal fatigue experiment

The temperature difference and the pressure are set to 100°C and 7.5 MPa respectively, which corresponds to a relative density difference $\delta\rho=\Delta\rho/\rho_{min}$ of ca. 6%. Table 1 lists the parameters for the geometry. The computational domain ranges from 3 diameters upstream, in both branch and main pipe, to 20 diameters downstream of the main pipe. The inlet flow is considered to be fully developed turbulent pipe flow. The domain of the intersecting pipes is modelled only with sharp edges. The pipe wall material is stainless steel 316L which has a density of ρ_S = 8000 kg/m^3, heat capacity of $c_{p,S}$ = 500 J/kg-K and heat conductivity of λ_S = 15 W/m-K. The Grashof number is of the order of $1\cdot10^9$. Therefore, the Richardson number Ri = Gr/Re^2 around unity, which indicates that strong buoyancy effects have to be expected. The gravity is set to 9.81 m/s^2 in negative z direction. Two cases are simulated. First, an adiabatic boundary condition case (A) without a solid domain is calculated. The second test case is a coupled fluid-solid simulation (C).

Pipe (Stream wise flow direction)		Main (x-direction)		Branch (y-direction)
Inner pipe diameter - [m]	$d = d_1$	0.0718	d_2	0.0389
Wall thickness - [m]	b_1	$8.55\cdot10^{-3}$	b_2	$4.7\cdot10^{-3}$
Temperature - [°C]	T_1	120	T_2	20
Massflow rate – [kg/s]	$\dot{m}_1$	0.4	$\dot{m}_2$	0.1
Reynolds number – [1]	Re_1	30300	Re_2	3300
Prandtl number – [1]	Pr_1	1.44	Pr_2	6.94

Table 1 Geometry and flow parameter

3. Physical models

Large-eddy simulation solves large scale turbulence directly for which no turbulence model is required. Small scale turbulence below the grid filter width Δ is usually assumed to be nearly isotropic and simple turbulence models, such as the algebraic mixing length models, are mainly applied. The general filtered Navier-Stokes equations and the energy equation are:

$$\frac{\partial}{\partial x_i}\left(\rho\bar{u}_i\right)=0 \tag{1}$$

$$\frac{\partial}{\partial t}\left(\rho\bar{u}_i\right)+\frac{\partial}{\partial x_j}\left(\rho\bar{u}_i\bar{u}_j\right)=\frac{\partial}{\partial x_j}\left[\mu\left(\frac{\partial\bar{u}_i}{\partial x_j}+\frac{\partial\bar{u}_j}{\partial x_i}\right)-\frac{2}{3}\mu\frac{\partial\bar{u}_k}{\partial x_k}\delta_{ij}\right]-\frac{\partial\bar{p}}{\partial x_i}-\frac{\partial\tau_{ij,SGS}}{\partial x_j}+\rho g_i \tag{2}$$

$$\frac{\partial}{\partial t}\left(\rho\overline{T}\right)+\frac{\partial}{\partial x_j}\left(\rho\overline{u}_j\overline{T}\right)=\frac{\partial}{\partial x_j}\left[\frac{\mu}{\mathrm{Pr}}\frac{\partial\overline{T}}{\partial x_j}-\tau_{\Theta j,SGS}\right] \tag{3}$$

These equations take buoyancy force into account while the density is defined as a polynomial function of temperature. The subgrid-scale shear stress components τ_{ij} in (2) need to be modeled by a subgrid-scale (SGS) model. Because isotropic turbulence is assumed for small scale turbulence the most utilized SGS models are based on the mixing length hypothesis. The SGS shear stress τ_{ij} is modeled as follows:

$$\tau_{ij,SGS}=-2\mu_t\left(\overline{S}_{ij}-\frac{1}{3}\overline{S_{kk}}\delta_{ij}\right) \tag{4}$$

In the Smagorinsky-Lilly model the subgrid-scale turbulent viscosity μ_t depends on the strain rate $S_{ij,}$, the cell volume V and the model constant C_S. The linear function of the length scale containing Kármán constant $\kappa = 0.41$ and the wall distance d ensure correct wall behavior in the near wall region.

$$\mu_t=\rho(\min(\kappa d,C_S\Delta)^2\sqrt{2\overline{S}_{ij}\overline{S}_{ij}} \tag{5}$$

$$\overline{S}_{ij}=\frac{1}{2}\left(\frac{\partial\overline{u}_i}{\partial x_j}+\frac{\partial\overline{u}_j}{\partial x_i}\right)\quad;\quad\Delta=V^{1/3} \tag{6}$$

The modified dynamic Smagorinsky-Lilly model by Germano [9] used in the presented simulation dynamically calculates C_S which is limited between 0 and 0.23. The turbulent heat flux also has to be modeled as follows:

$$\tau_{\Theta j,SGS}=-\frac{\mu_t}{\mathrm{Pr}_t}\frac{\partial\overline{T}}{\partial x_j} \tag{7}$$

The default empirical value for the turbulent Prandtl number is $\mathrm{Pr_t}$=0.85. Furthermore, the near wall region is treated according to the blending function by Kader [10], which allows reasonable coverage of the buffer layer, for which the logarithmic wall function alone would fail.

4. Numerical Grid

The main restriction for a LES grid is given by requirements for the near wall resolution and the maximum allowed aspect ratio. Several suggestions for proper resolution of the near-wall region can be found in literature for both wall-resolved LES and LES utilizing wall functions. The wall function LES estimates the velocity of the first cell centre which in the turbulent region of the boundary layer, whereas wall resolved LES requires a very fine grid in order to resolve the viscous sublayer. Fröhlich [11] has summarized recommendations for fully resolved LES made by Nikuradse (less restrictive), Sagaut (most restrictive) and from his own work shown in Table 2. The length, height and width of the first cell from the wall surface are denoted as Δx, Δy and Δz respectively. The superscript "+" indicate a dimensionless entity according to $\Delta y^+=\Delta y\cdot u_\tau/\nu$ with

friction velocity u_τ and kinematic viscosity ν. The subscript "1" indicates the first cell centre away from the wall.

	Wall resolved LES			Wall function LES		
	Δx^+	Δy^+	Δz^+	Δx^+	Δy^+	Δz^+
Sagaut	10	2	5	-	20-200	-
Nikuradse	100	2	40	100-600	30-150	100-300
Fröhlich	50	2	15	δ/5	< δ/5	$= \Delta y^+$

Table 2 Overview of recommended near wall resolution. [11]. (δ – boundary layer thickness)

	Δx^+	$\Delta y^+ = 2 \cdot y_1^+$	Δz^+
Main pipe	40 – 100	20	40

Table 3 Non-dimensional parameters of wall adjacent cell of the grid used in this simulation, based on the main pipe bulk flow and fully developed turbulent pipe flow.

Comparing Table 2 and Table 3 shows that the design parameter of the grid used in this simulation is fairly coarse and lies between the requirements of a fully resolved LES and the less restrictive requirements for the wall-function approach. Estimations in Table 2 are based on fully developed turbulent pipe flow conditions. When running the simulation, the non-dimensional wall distance of the first cell center $y_1^+ = ½\ \Delta y^+$ varies between 1 and 10 downstream of the intersection. The grid contains ca. 5 million cells for both fluid and solid region combined. The wall region contains 30 cells for the wall thickness with geometrically growing cell sizes towards the outer wall surface. The first wall cell has a thickness of $\Delta y_{solid}^+ = 1$.

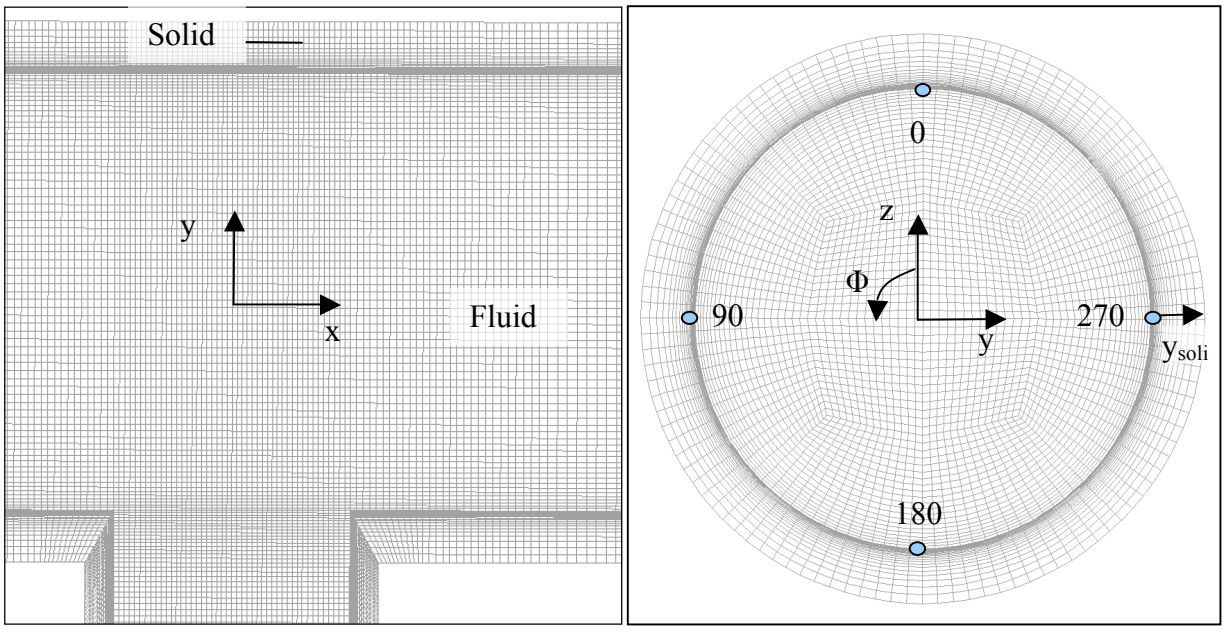

Figure 1 numerical grid, xy-plane, z=0 (left) , yz-plane-plane (right)

4.1 Numerical methods

For velocity-pressure coupling the PISO scheme and the non-iterative time advancement option are chosen in ANSYS FLUENT 12.1. The 2nd order pressure scheme is applied along with the central differencing scheme for the momentum equation and the QUICK scheme for the energy equation. Furthermore, the temperature depending fluid properties are implemented as polynomials for a system pressure of 7.5MPa according to the IAPWS Formulation for water and steam from 1995 [12]. For the conjugate heat transfer simulation the coupled boundary condition is applied for the fluid solid interface which assures continuity of the temperature field and the normal temperature gradient. The outer pipe wall is set to an adiabatic wall. The boundary condition for the wall around the pipe inlet and the outlet are set as symmetry boundary conditions. The time step is set to 1ms which results in a maximum cell Courant number of CFL < 0.71. The total physical simulation time for the coupled simulation was t ≈ 125 seconds. Statistics are taken from second ca. t ≈ 85s when the solution begins to be statistically steady. Data for the spectral analysis are stored for the last 24s of physical simulation time. An instantaneous flow field of the adiabatic solution is used as initial condition for the fluid region. A steady state solution for the solid region based on the mean temperature distribution of the adiabatic solution for the inner pipe wall is applied as the initial condition of the solid domain. This is assumed to be the fastest way to reach a statistically steady state inside the wall domain since the adiabatic solution was already available.

5. Simulation Results

The temperature (instantaneous, mean and RMS values) is presented in a normalized form and is defined as follows:

$$T^* = \frac{T - T_{cold}}{T_{hot} - T_{cold}} \quad ; \quad T^*_{mean} = \overline{T^*} = \frac{\sum_{i=1}^{N} T^*_i}{N} \quad ; \quad T^*_{rms} = \sqrt{\overline{\left(T^* - \overline{T^*}\right)}} \tag{8}$$

Figure 2 to Figure 4 show the general characteristics of the T-junction flow. With strong stratification it is a mixed convection flow. Cold fluid from the branch pipe shoots down very quickly. The lateral momentum of the cold flow results in a wavy movement as the fluid flows downstream (Figure 2 and Figure 3).

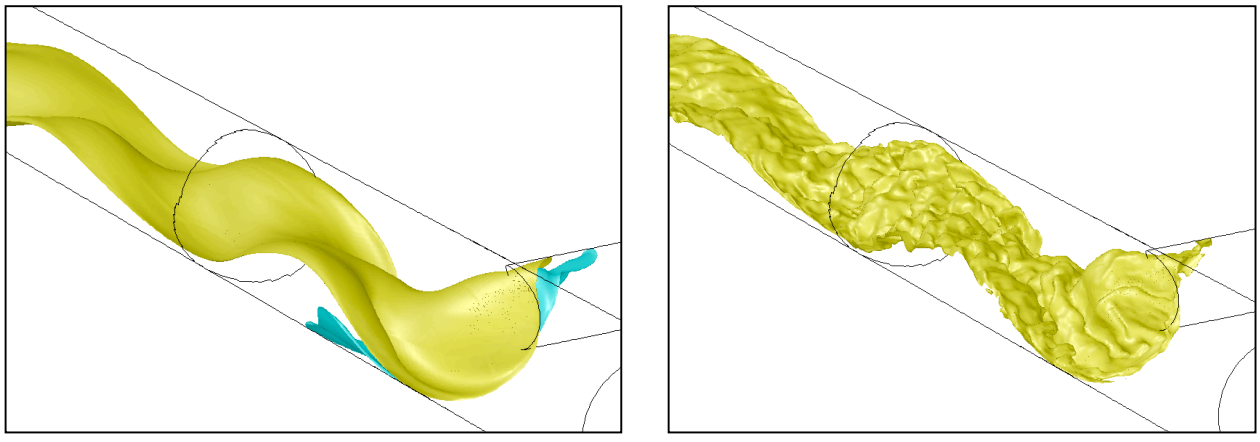

Figure 2 Isosurfaces of the mean (left) and instantaneous (right) values of T* = 0.7

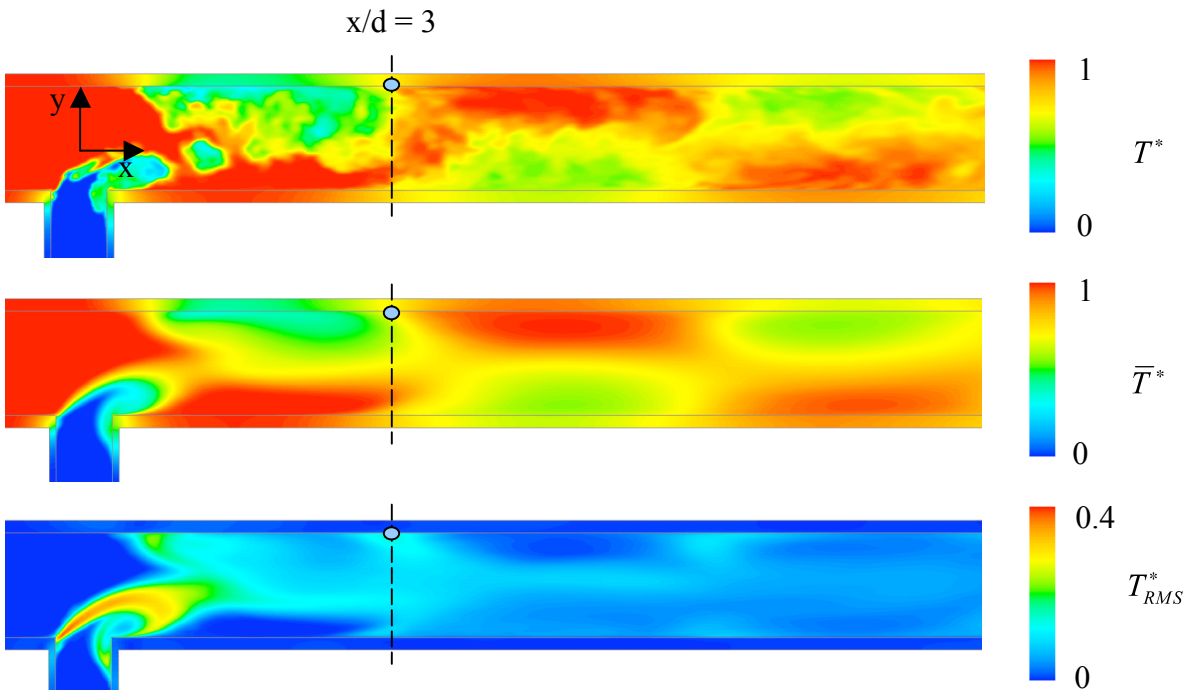

Figure 3 Contours of instantaneous (top), mean (middle) and RMS (bottom) values of T* in the xy-plane. The line (--) and the dot indicate the location investigated in more detail (x/d = 3, Φ =270°).

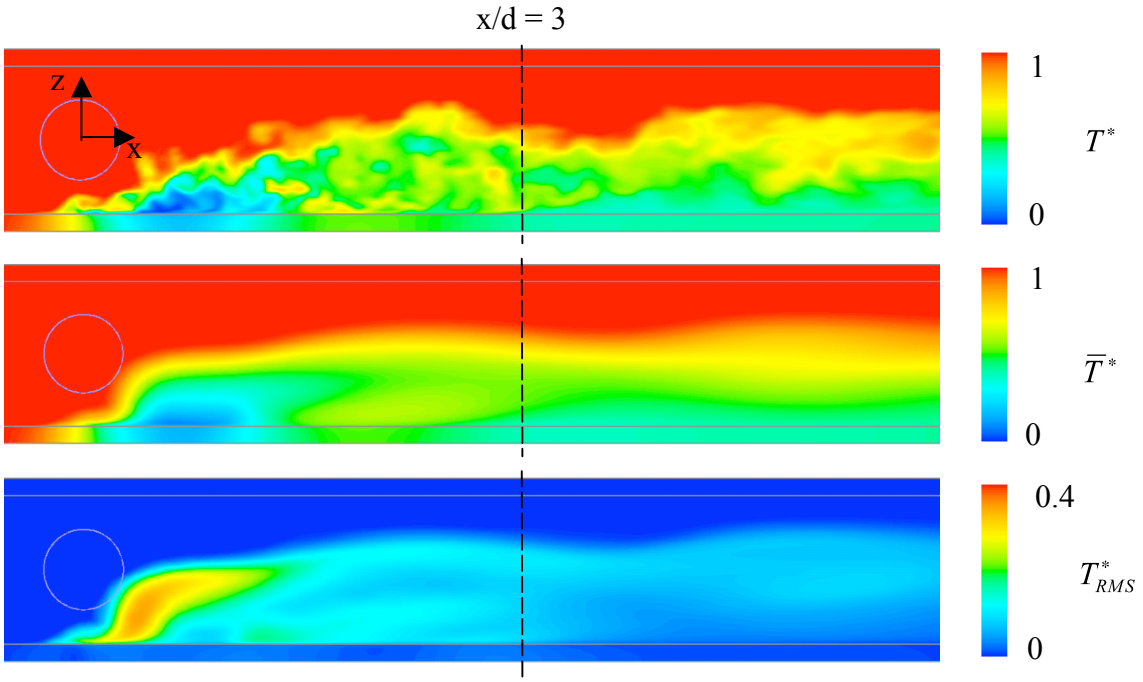

Figure 4 Contours of instantaneous (top), mean (middle) and RMS values (bottom) of T* in the xz-plane. The line (--) indicates the position x/d = 3, Φ =270°.

The stratification is very stable and the wavy character of the temperature isosurface is maintained until 20D downstream. The characteristic length between the local maxima of the stratification surface lies in between 5.5 - 5.8 diameter. The larges fluctuations occur directly at the intersection of the main and branch pipe and at the bottom of the T-junction (Figure 4). Due to buoyancy forces the hot fluid enters partly in the upper region of the branch pipe where large fluctuations can be found. The general flow pattern is steady in time, as demonstrated by the instantaneous temperature field at an arbitrary time step in Figure 2 (right).

5.1 Temperature Statistics

The mean value and RMS profiles for the coupled and the adiabatic solution is overlapping for the most part of the domain (Figure 6, y/d < 4.5). The near wall temperature RMS profiles, however, are highly affected by the unsteady heat flux (Figure 6). Thermal inertia of the wall material leads to significant damping of the RMS values at the fluid-solid interface and the nearest cells. Therefore, the wall surface is therefore subjected to only 20% to 50% of the temperature fluctuations, which are calculated for the adiabatic case (Figure 5 , Figure 6, and Figure 7).

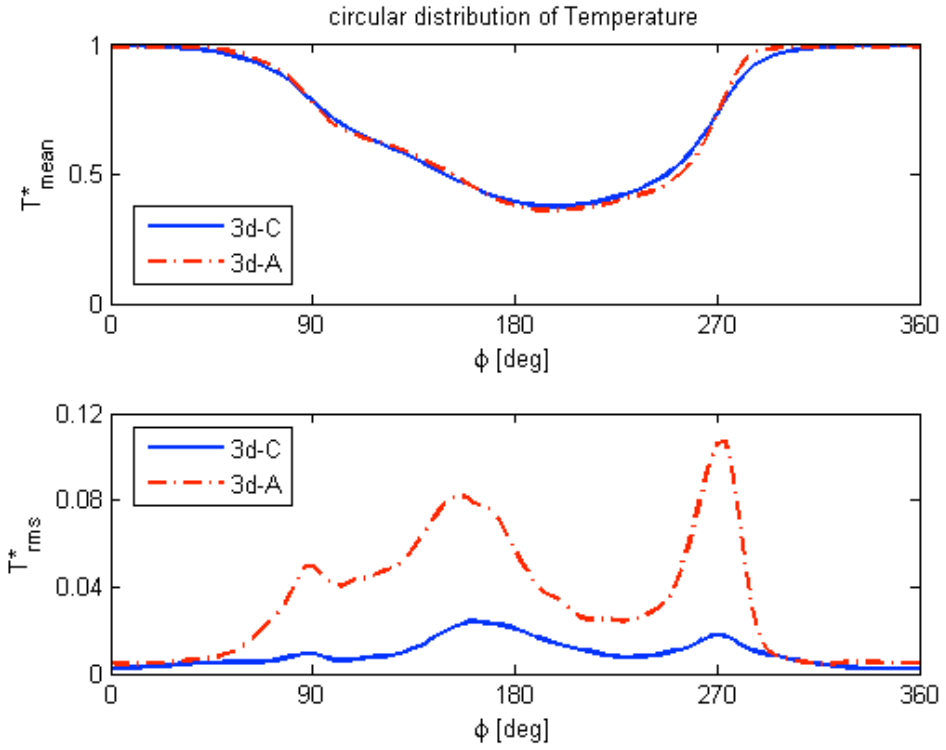

Figure 5 Circular distribution of mean (top) and RMS values (bottom) of normalized temperature. Comparison between coupled and adiabatic solution at x/d = 3.

The circular distribution in Figure 5 shows almost complete overlap of the adiabatic case and the coupled case. The damping factor for the temperature fluctuations from the fluid to the wall surface (coupled case) is not uniform but changes significantly around the pipe.

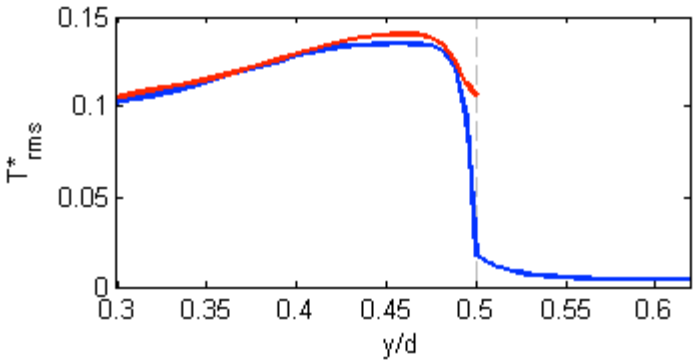

Figure 6 Horizontal temperature RMS profile near the wall at x/d = 3 for the adiabatic case (red) and the coupled case (blue)

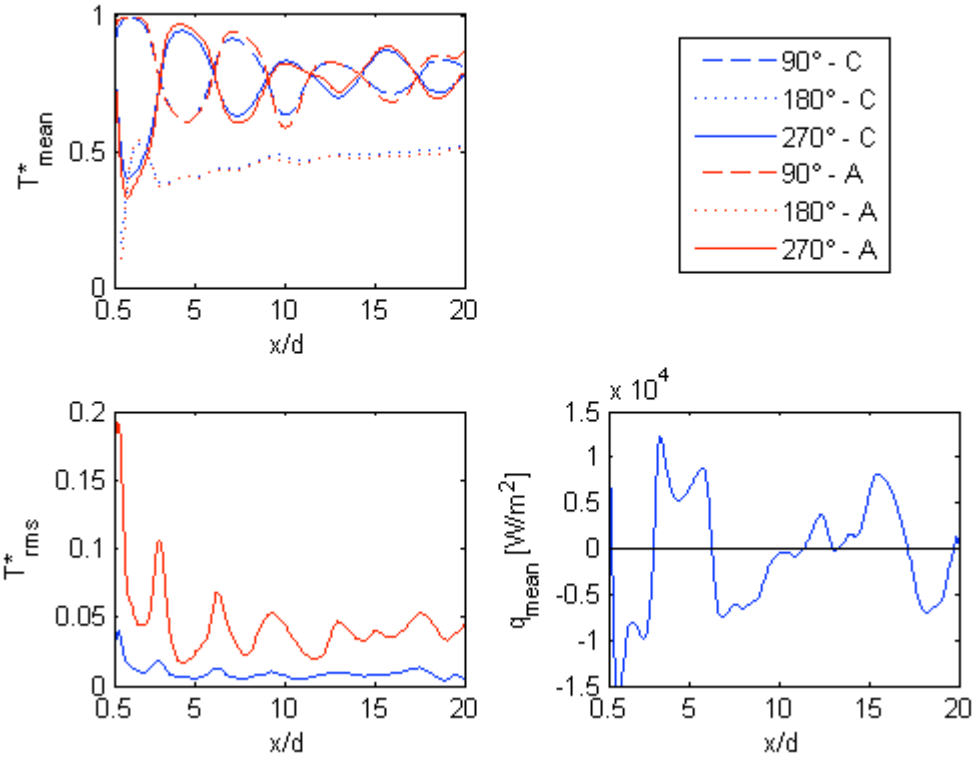

Figure 7 Distribution of the mean (top left), the RMS values (bottom left) of normalized Temperature and the total surface heat flux (bottom right). A- adiabatic, C – coupled

At x/d = 3 and Φ = 270° a local maximum for the temperature fluctuations (Figure 7 - bottom, left) corresponds to a very low value of mean surface heat flux q_{mean}. The time series of the heat flux in Figure 8 (blue line), however, shows that the amplitudes of the fluctuation are large. For x/d=3 the temperature gradient along the circumferential direction is the largest at Φ = 270° (Figure 5). At this point, the gradient of the mean temperature through the wall thickness is almost zero. Therefore, the mean temperature of the wall surface is the same as the near wall fluid. Hence, little or no heat is exchanged in the mean sense.

The mean q_{mean} is non-zero where the wall surface has a different mean value than the near wall fluid due to effective heat conduction in the wall (Figure 8, Φ = 290°). However, the fluctuations are vastly reduced.

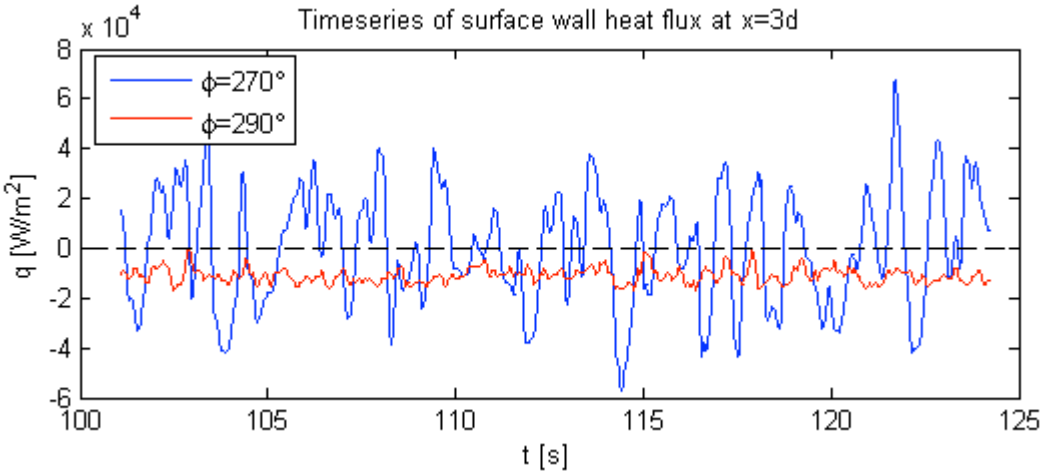

Figure 8 Time series of total surface heat flux for x/d = 3 for two different angles.

5.2 Frequency analysis

Figure 9 shows the time series of the wall temperature fluctuations (blue) at x/d = 3 and Φ = 270° for the coupled simulation. The amplitudes of the temperature at 25% wall distance (red) are down to ca. 30% compared to the amplitudes at the inner wall surface accompanied with a delay of 0.5 to 1s. The temperature spectrum in Figure 10 is taken for a time span of 24 seconds. The near wall temperature fluctuations in the fluid (black) are damped when reaching the wall surface for all frequencies. Frequencies above 1Hz are reduced significantly more than lower frequencies. As expected, within the wall region the damping increases with the frequency. No damping occurs between the inner wall surface and 25% wall thickness for f = 0.1Hz.

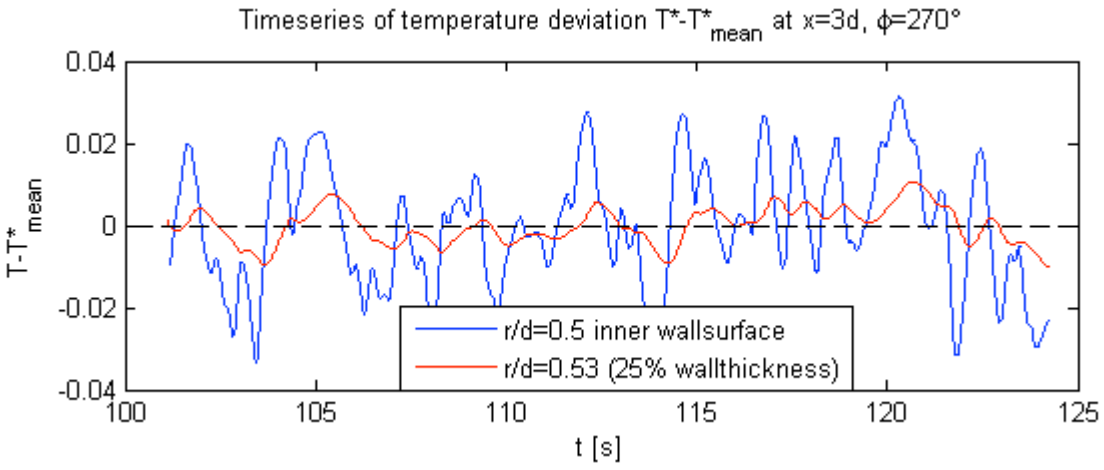

Figure 9 Time series of temperature fluctuations at x = 3d at wall surface and inside the wall material.

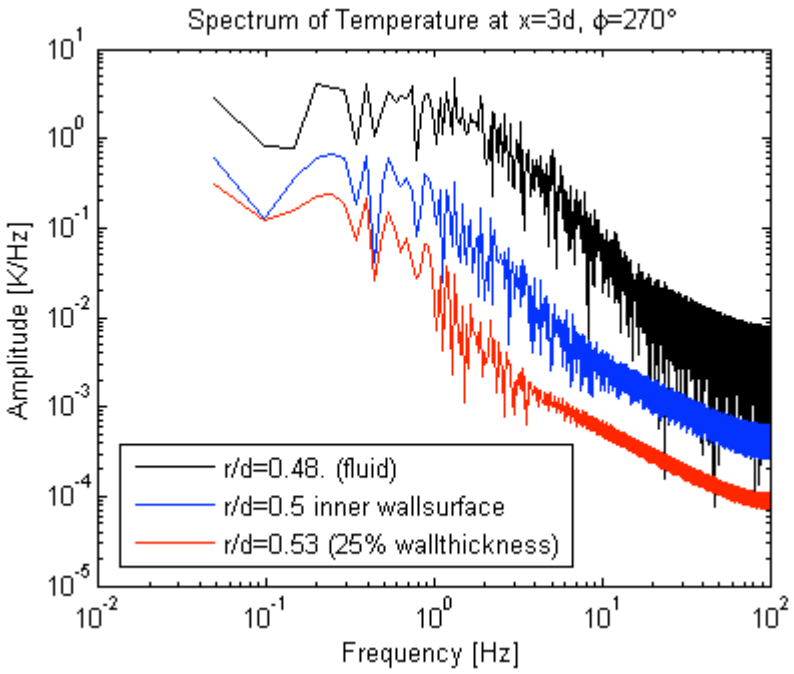

Figure 10 Spectrum of Temperature for near wall region, wall surface and inside the wall. r/d indicates the radial position.

6. Conclusion

A blind Conjugate heat transfer LES simulation of a T-junction mixing flow is presented based on realistic power plant condition. A stable stratification is established in less than a diameter downstream due to the large temperature. The downstream flow is characterized by wavy movement and temperature distribution. This overall flow pattern is induced by the lateral momentum of the cold water and steady in time (i.e. local peaks keep their position). Reduced mixing due to immediate and strong stratification maintains this flow pattern down to the end of the computational domain. Heat transfer fluctuations are large, where large RMS values of temperature fluctuation occurs. Above and below the stratification line heat transfer is less fluctuating with a significant net mean heat flux into the water (cold region) and into the wall (hot region) can be observed. This is due to lateral heat conduction in the wall material.

LES methods still need to be validated for realistic power plant conditions. It was shown that the coupled simulation approach is helpful to understand the mechanisms of thermal fatigue in T-junctions which are related to stratification and unsteady heat transfer effects.

7. References

[1] S. Chapuliot,C. Gourdin, T. Payen, J.P. Magnaud and A. Monavon, “Hydro-thermal-mechanical analysis of thermal fatigue in a mixing tee”, Nuclear Engineering and Design, Vol. 235, 2005, pp. 575-596

[2] K.-J. Metzner and U. Wilke, “European THERFAT project – thermal fatigue evaluation of piping system”, *Nuclear Engineering and Design*, Vol. 235, 2005, pp. 473-484

[3] P. Coste et al. , “Large Eddy Simulation of a Mixing-T Experiment”, Proceedings of ICAPP’06, Reno, Nevada, USA, 2006, June 4-8

[4] J. Westin et al., "Experiments and unsteady CFD-calculations of thermal mixing in a T-junction", Proceedings of CFD4NRS, Munich, Germany, 2006

[5] S.T. Jayaraju, E.M.J. Komen and E. Baglietto, "Suitability of wall-function in Large Eddy Simulation for thermal fatigue in a T-junction", *Nuclear Engineering and Design*, Vol. 240, 2010, pp. 2544-2554

[6] M.H.C. Hannink and A.K. Kuczaj et al., "A Coupled CFD-FEM stratefy to predict thermal fatigue in mixing tees of nuclear reactors", Proceedings of the EUROSAFE, Paris, France, November 3-4, 2008

[7] S. Kuhn et al. "Computational study of conjugate heat transfer in T-junctions*", Nuclear Engineering and Design*, Vol. 240, 2010, pp. 1548-1557

[8] R.J.A. Howard and Thomas Prasutto, "The effect of Adiabatic and Conducting Wall Boundary Conditions on LES of a Thermal Mixing Tee*",* Proceedings of the NURETH-13, Kanazawa City, Ishikawa Prefecture, Japan, September 27-October 2, 2009.

[9] M. Germano, U. Piomelli, P. Moin and W.H. Cabot, "A dynamic subgrid-scale viscosity model", *Phys. Fluid*, A3, 1991, pp. 1760-1765

[10] B. Kader, "Temperature and Concentration Profiles in Fully Turbulent Boundary Layers ", Int. *J. Heat Mass Transfer*, 24(9), 1981, pp. 1541-1544

[11] J. Fröhlich, "Large Eddy Simulation turbulenter Strömungen", Teubner, 2006

[12] W. Wagner and A. Pruss, "The IAPWS Formulation 1995 for the Thermodynamic Properties of Ordinary Water Substance for General and Scientific Use," *J. Phys. Chem. Ref. Data*, 31, 2002, pp. 387-535